Inorganica Chimica Acta 512 (2020) 119887

Contents lists available at ScienceDirect

Inorganica Chimica Acta

journal homepage: www.elsevier.com/locate/ica

Research paper

Synthesis and structural characterization of facile ruthenium(II) hydrazone complexes: Efficient catalysts in α-alkylation of ketones with primary alcohols via hydrogen auto transfer

Subbarayan Vijayapritha[a], Kaliyappan Murugan[a], Periasamy Viswanathamurthi[a,*], Paranthaman Vijayan[a], Chinnasamy Kalaiarasi[b]

[a] Department of Chemistry, Periyar University, Salem 636 011, India
[b] Department of Physics, Periyar University, Salem 636 011, India

ARTICLE INFO

Keywords:
Ruthenium(II) catalyst
Hydrazino benzothiazole
Crystal structure
α-alkylation
Borrowing hydrogen

ABSTRACT

As a immersion for development of new complexes, new Ru(II) complexes (**1**–**3**) supported by benzothiazole hydrazine Schiff bases of the type [Ru(SAL-HBT)(CO)($AsPh_3$)$_2$], [Ru(VAN-HBT)(CO)($AsPh_3$)$_2$] and [Ru(NAP-HBT)(CO)Cl($AsPh_3$)$_2$] [SAL-HBT = (salicyl((2-(benzothiazol-2yl)hydrazono)methylphenol)), VAN-HBT = 2-((2-(benzothiazol-2-yl)hydrazono)methyl)-6 methoxyphenol) and NAP-HBT = naphtyl-2-((2-(benzothiazol-2-yl) hydrazono)methyl phenol)] were synthesized. Their identities have been established by satisfactory elemental analyses, various spectroscopic techniques (IR, (^{1}H, ^{13}C) NMR) and also mass spectrometry. The ruthenium(II) ion exhibits a hexa coordination with distorted octahedral geometry. In complexes **1** and **2**, the ligand coordinated as dianionic tridentate fashion by forming NˆN donor five member and NˆO donor six member chelate rings. However, in complex **3**, the ligand coordinated as monoanionic bidentate fashion by forming NˆN donor five-membered ring. The new ruthenium(II) carbonyl complexes were successfully applied as catalysts in α -alkylation of aliphatic and aromatic ketones with alcohols via borrowing hydrogen strategy. Various parameters such as base, solvent, temperature, time and catalyst loading on the catalytic activity were analyzed. From the results, the catalyst **1** was found to be the best catalyst for α-alkylation reaction to obtain excellent yield. The catalytic system has a broad substrate scope, which allows the synthesis of α-alkylated ketones in mild reaction conditions with low catalyst loading under air atmosphere.

1. Introduction

The design of ligand can lead to pioneering metal chemistry since the nature of the multidentate ligands has a profound effect on the coordination chemistry of a metal complex. In this connection, many research groups have focused their attention on Schiff base ligands due to their rich coordination chemistry [1–3]. Particularly, Schiff base ligands own their main advantages like easily accessible under smooth conditions, very much facilitative to adjust their structures and ability to change chemo-physical properties through the incorporation of some additional functional groups. The resulting complexes exhibit numerous applications in catalysts [4], pharmaceuticals [5] and magnetic materials [6]. Generally special attention has been directed to the use of multidentate Schiff base ligands including hydrazones having both hard and soft donor atoms (e.g. N_2S_2 or XNS, X = N, O or S) because of their coordination versatility [7] and remarkable applications in catalytic [8] and biological sciences [9]. Such types of ligands were synthesized by appropriate functionalization of precursor carbonyl compounds. The recent report shows that hydrazone Schiff bases designed from heterocyclic hydrazine framework attract considerable attention as versatile ligands with respect to their variable coordination behavior [10]. Apart from the ligand, the properties of the coordination compounds, particularly catalytic activities depend on the central metal also. Several transition metal complexes containing Schiff bases reported as catalysts in many organic transformations [8,11].

On the other hand, transition metal complexes catalyzed construction of carbon–carbon bond by alkylation of ketones has attracted prominent place in organic chemistry [12]. Generally, such an alkylation can be realized by the reactions of enolates or enamines derived from ketones with carbon electrophiles, such as alkyl halides [13,14]. However, usage of carcinogenic halogen substrates, necessary pre functionalization procedure and the formation of stochiometric amount

* Corresponding author.
E-mail address: viswanathamurthi@gmail.com (P. Viswanathamurthi).

https://doi.org/10.1016/j.ica.2020.119887
Received 18 May 2020; Received in revised form 10 July 2020; Accepted 10 July 2020
Available online 14 July 2020
0020-1693/

of unwanted salts as waste at the end of the reaction minimizes the utility of conventional synthesis [15]. To circumvent the above drawbacks, development of an alternative protocol is essential to achieve the related objective. In recent years advancement in homogeneous catalysis and catalyst design has led to the development of an alternative protocol referred as "borrowing hydrogen" and also as "hydrogen autotransfer" method in which environmentally benign, inexpensive and readily available alcohols were used as alkylating partners for alkylation reactions [16]. The alkylation reactions are in accordance with sustainable development in views of economy and environment since such reaction release of water as the only byproduct in addition to highly atom economical [17,18].

Following on from the pioneering work conducted by Grigg and co-workers [19], hydrogen borrowing has been investigated extensively by numerous research groups, and several reviews have been published pertaining to alkylation reactions involving auto transfer hydrogenation using alcohols [15]. A variety of ruthenium and iridium metal catalysts, including $RuHCl(CO)(PPh_3)_3$, $RuCl_2(PPh_3)_3$, $[Ir(cod)Cl_2]_2/PPh_3$, Pd/C, and $RuCl_2(DMSO)_4$, have been designed for the α-alkylation of carbonyl compounds using alcohols and these reactions were carried out in the presence of a base and/or hydrogen acceptor system [20]. Kaneda and co-workers developed hydrotalcite-supported ruthenium heterogeneous catalysts, which required prolonged heating at high temperature (180 °C, 20–30 h) in addition to the use of alkylating alcohols as solvents [21]. Ruthenium(II) half sandwich complexes developed for this transformation exhibited poor catalytic activity and provided partial hydrogenation, resulting in the presence of unsaturated vinyl nitrile predominantly in the mixture of products [22]. Min Zhang and co workers [23] employed an easily available $[Ru(p\text{-cymene})Cl_2]_2$/Xantphos/*t*-BuOK catalyst system for α-alkylation of ketones using pyridyl methanol as the alkylating reagents. The synthetic protocol allows synthesizing a wide range of α-pyridyl methylated ketones in reasonable to excellent isolated yields with high atom-efficiency. Zhu group [24] reported NNN pincer Ru(II) complex as catalyst for α-alkylation of ketones with alcohols including (hetero)aryl- or alkyl-ketones and alcohols. This protocol enables the facile synthesis of donepezil drug in 83% yield. Glorius and co workers [25] reported ruthenium(II) NHC catalyst for α-alkylation of methylene ketones including direct one-step synthesis of donepezil drug. Ruthenium pyridonate catalysts developed by Chen's group [26] show TOF values up to 3680 h^{-1} for α-alkylation of ketones. Our own group has also successful in applying the ruthenium carbonyl complexes [27] to couple a wide range of amines, diamines and alcohols together.

Based on the above facts and in continuing our efforts to study the coordination behavior of complexes and exploit new catalytic system, this work describes synthesis of new Schiff base from hydrazino benzothiazole and salicylaldehyde/*o*-vanillin/2-hydroxy-1-naphthaldehyde and their ruthenium(II) complexes (**1–3**). The chelating behavior of ligands with ruthenium ion was extensively investigated using various spectroscopy techniques and their solid-state structures were established by single-crystal XRD. The catalytic properties of the new Ru(II) complexes (**1–3**) have been screened in α-alkylation of ketones with alcohols.

2. Experimental

2.1. General strategy

Commonly available $RuCl_3{\cdot}3H_2O$ was used as supplied from Sigma Aldrich. All chemicals and solvents were acquired from Merck or Aldrich. Thin-layer chromatography (Merck 1.05554 aluminum sheets precoated with silica gel 60 F254) was used for reaction observance and the spots were visualized with UV light at 254 nm or under iodine. Column chromatography refinement was done for the complexes using silica gel (200–400 mesh). Melting points were checked in open capillary tubes on a Technico micro heating table and are uncorrected. Infrared spectra of the compounds were obtained in the range of 4000–400 cm^{-1} using Bruker alpha FT-IR spectrophotometer in ATR mode. ^1H (400 MHz) and ^{13}C (100 MHz) NMR spectra were recorded in DMSO-d_6 or $CDCl_3$ at room temperature with a Bruker AV400 instrument using internal standard tetramethylsilane. Quadrupole time-of-flight Micro Analyzer (Shimadzu) mass spectrometry was used to measure electrospray ionization mass spectra (ESI) of compounds at SAIF, Panjab University, Chandigarh. Elemental analysis (C, H, N and S) were done on a Vario EL III elemental analyzer. The hydrazone ligands were synthesized according to a previously published method with slight modifications [28]. The ruthenium precursor $[RuHCl(CO)(AsPh_3)_3]$ was synthesized based on the standard procedure [29].

2.2. Synthesis of ligands

The following common procedure were used to synthesis the ligands. Typically an ethanol solution (20 mL) of substituted aldehyde (1 mmol) was added to 2-hydrazino benzothiazole (1 mmol) and the resulting mixture was stirred at room temperature for 5 h. The completion of the reaction was checked by thin layer chromatography (TLC) and then the resulting white precipitate was filtered, washed using diethyl ether and air dried.

2.2.1. Synthesis of salicyl((2-(benzothiazol-2-yl)hydrazono)methyl phenol (SAL-HBT)

The reaction of salicylaldehyde (0.122 g, 1 mmol) and 2-hydrazino benzothiazole (0.165 g, 1 mmol) was carried out for synthesis of the ligand SAL-HBT. Yield: 88%. M.p.: 243 °C. Anal. Calcd for $C_{14}H_{11}ON_3S$: C, 62.43; H, 4.12; N, 15.60; S, 11.91%. Found: C, 62.56; H, 4.23; N, 15.79; S, 12.03%. IR (KBr, ν cm^{-1}): 3352 (br, ν_{OH}), 3123 (w, ν_{NH}), 1573 + 1467 (s, $\nu_{C=N}$ + ν_{C-N}), 747 (s, $\nu_{C\text{-}S}$). ^1H NMR (400 MHz, $CDCl_3$, ppm): 10.86 (s, 1H, OH), 8.38 (s, 1H, −CH=N), 7.59–6.89 (m, 4H, Ar H), 4.25 (s, 1H, NH). ^{13}C NMR (100 MHz, $CDCl_3$, ppm): 167.1 (S-C=N), 148.7 (C=N), 133.6 (Ar C), 131.3 (Ar C), 126.7 (Ar C), 124.1 (Ar C), 122.4 (Ar C), 121.8 (Ar C), 119.8 (Ar C), 116.5 (Ar C). ESI mass (*m/z*) calcd. for $C_{14}H_{11}N_3OS$, 269.3; Found, 270.4 $[M+H]^+$.

2.2.2. Synthesis of 2-((2-(benzothiazol-2-yl)hydrazono)methyl)-6-methoxyphenol (VAN-HBT)

The reaction of *o*-vanillin (0.152 g, 1 mmol) and 2-hydrazino benzothiazole (0.165 g, 1 mmol) was carried out for synthesis of the ligand VAN-HBT. Yield: 87%. M.p.: 210 °C. Anal. Calcd. for $C_{15}H_{13}O_2N_3S$: C, 60.18; H, 4.38; N, 14.04; S, 10.71%. Found: C, 60.27; H, 4.54; N, 14.16; S, 10.83. IR (KBr, ν cm^{-1}): 3574 (br, ν_{OH}), 3145 (w, ν_{NH}), 1609 + 1469 (s, $\nu_{C=N}$ + ν_{C-N}), 773 (s, $\nu_{C\text{-}S}$). ^1H NMR (400 MHz, $CDCl_3$, ppm): 11.04 (s, 1H, OH), 8.39 (s, 1H, −CH=N), 7.51–6.84 (m, 7H, Ar H), 4.51 (s, 1H, NH), 3.93 (s, 3H, $-OCH_3$). ^{13}C NMR (100 MHz, $CDCl_3$, ppm): 167.1 (S-C=N), 153.3 (Ar C), 151.0 (Ar C), 148.4 (Ar C), 146.7 (C=N), 126.3 (Ar C), 125.1 (Ar C), 124.1 (Ar C), 122.0 (Ar C), 120.8 (Ar C), 119.4 (Ar C), 117.5 (Ar C), 56.3 (Ar C); ESI mass (*m/z*) calcd. for $C_{15}H_{13}N_3O_2S$, 299.3; Found, 300.3 $[M + H]^+$.

2.2.3. Synthesis of naphtyl-2-((2-(benzothiazol-2-yl)hydrazono)methyl phenol (NAP-HBT)

The reaction of 2-hydroxy-1-naphthaldehyde (0.172 g, 1 mmol) and 2-hydrazino benzothiazole (0.165 g, 1 mmol) was carried out for synthesis of the ligand NAP-HBT. Yield: 84%. M.p.: 230 °C. Anal. Calcd for $C_{18}H_{13}ON_3S$: C, 67.69; H, 4.10; N, 13.16; S, 10.04%. Found: C, 67.81; H, 4.26; N, 13.29; S, 10.19%. IR (KBr, ν cm^{-1}): 3630 (br, ν_{OH}), 3066 (w, ν_{NH}), 1582 + 1471 (s, $\nu_{C=N}$ + ν_{C-N}), 774 (s, $\nu_{C\text{-}S}$). ^1H NMR (400 MHz, $CDCl_3$, ppm): 10.65 (s, 1H, OH), 8.10 (s, 1H, −CH=N), 7.96–7.22 (m, 10H, Ar H), 4.35 (s, 1H, NH). ^{13}C NMR (100 MHz, $CDCl_3$, ppm): 168.4 (S-C=N), 156.2 (Ar C), 148.4 (Ar C), 142.4 (C=N), 132.6 (Ar C), 129.2 (Ar C), 128.5 (Ar C), 128.1 (Ar C), 126.0 (Ar C), 125.8 (Ar C), 123.9 (Ar C), 122.1 (Ar C), 121.1 (Ar C), 108.6 (Ar C), 105.6 (Ar C). ESI mass (*m/z*) calcd. for $C_{18}H_{13}N_3OS$, 319.3; Found, 320.3 $[M+H]^+$.

2.2.4. Synthesis of new ruthenium(II) complexes

The following common method has been used to synthesis all the complexes. The starting complex [RuHCl(CO)($AsPh_3$)$_3$] (0.1 mmol) was added to ethanol-chloroform (20 mL, 1:1 v/v) solution of corresponding ligand (0.1 mmol) and refluxed for 24 h in air. During the course of reaction, color of the reaction mixture was changed. The thin layer chromatography (TLC) was used to check progress of the reaction. When the reaction completes, the solvents were removed using a rotary evaporator and the resulting crude product was thoroughly washed with cold ethanol and diethyl ether then purified by recrystallization using solvents chloroform and petroleum ether.

2.2.5. Synthesis of [Ru(SAL-HBT)(CO)($AsPh_3$)$_2$] (1)

The ligand SAL-HBT (0.026 g, 0.1 mmol) was reacted with [RuHCl(CO)($AsPh_3$)$_3$] (0.105 g, 0.1 mmol) for the synthesis of complex **1**. Yield: 80%. Color: Yellow. M.p.: 185 °C. Anal. Calcd. for $C_{51}H_{39}As_2O_2N_3RuS$: C, 60.72; H, 3.90; N, 4.17; S, 3.18%. Found: C, 60.88; H, 4.06; N, 4.31; S, 3.29%. IR (ATR, cm^{-1}): 1561 + 1459 (m, $\nu_{C=N} + \nu_{C-N}$); 741 (s, ν_{C-S}); 1948 (s, ν_{CO}), ^{1}H NMR (400 MHz, $CDCl_3$, ppm): 8.16 (s, 1H, −CH=N), 7.82 (d, J = 8 Hz, 1H, Ar H), 7.70–7.61 (m, 6H, Ar H), 7.52–7.40 (m, 9H, Ar H), 7.33–6.99 (m, 16H, Ar H), 6.88–6.79 (td, J = 4 Hz, 2H, Ar H), 6.29 (d, J = 8 Hz, 1H, Ar H), 6.12 (t, J = 4 Hz, 2H, Ar H). ^{13}C NMR (100 MHz, $CDCl_3$, ppm): 205.2 (CO), 164.4 (–HC=N), 158.6 (N=C-N), 147.7 (Ar C), 139.5 (Ar C), 133.8 (Ar C), 131.4 (Ar C), 130.6 (Ar C), 128.8 (Ar C), 125.9 (Ar C), 123.2 (Ar C), 121.9 (Ar C), 118.3 (Ar C), 117.0 (Ar C), 113.9 (Ar C), 127.6–117.8 (Ar C of $AsPh_3$); ESI: *m/z* calcd. for $C_{51}H_{39}$ $As_2O_2N_3RuS$, 1008.8; Found, 1010.0 $[M+2H]^+$. Single crystals of suitable for X-ray determination were grown by slow evaporation of chloroform-ethanol (1:1) solution of complex **1** at room temperature.

2.2.6. Synthesis of [Ru(VAN-HBT)(CO)($AsPh_3$)$_2$] (2)

The ligand VAN-HBT (0.029 g, 0.1 mmol) was reacted with [RuHCl(CO)($AsPh_3$)$_3$] (0.105 g, 0.1 mmol) for the synthesis of complex **2**. Yield: 78%. Color: Yellow. M.p.: 179 °C. Anal. Calcd. for $C_{52}H_{41}As_2O_3N_3RuS$: C, 60.12; H, 3.98; N, 4.04; S, 3.09%. Found: C, 60.21; H, 4.03; N, 4.12; S, 3.21%. IR (ATR, cm^{-1}): 1596 + 1458 (m, $\nu_{C=N} + \nu_{C-N}$); 762 (s, ν_{C-S}); 1951 (s, ν_{CO}), ^{1}H NMR (400 MHz, $CDCl_3$, ppm): 8.26 (s, 1H, −CH=N), 7.84 (t, J = 4 Hz, 3H, Ar H), 7.45–7.25 (m, 7H, Ar H), 7.21–6.93 (m, 21H, Ar H), 6.79 (d, J = 8 Hz, 1H, Ar H), 6.44(d, J = 4 Hz, 2H, Ar H), 6.02 (d, J = 4 Hz, 3H, Ar H), 3.86 (s, 3H, $-OCH_3$). ^{13}C NMR (100 MHz, $CDCl_3$, ppm): 205.2 (CO), 164.4 (–HC=N), 155.3 (N=C-N), 147.7 (Ar C), 143.7 (Ar C), 133.1 (Ar C), 130.7 (Ar C), 128.4 (Ar C), 125.6 (Ar C), 123.0 (Ar C), 122.0 (Ar C), 118.3 (Ar C), 116.8 (Ar C), 112.6 (Ar C), 56.1 (–OCH_3), 139.8–116.8 (Ar C of $AsPh_3$); ESI: *m/z* calcd. for $C_{52}H_{41}As_2O_3N_3RuS$, 1038.8; Found, 1040.0 $[M+2H]^+$.

2.2.7. Synthesis of [Ru(NAP-HBT)(CO)Cl($AsPh_3$)$_2$] (3)

The ligand NAP-HBT (0.031 g, 0.1 mmol) was reacted with [RuHCl(CO)($AsPh_3$)$_3$] (0.105 g, 0.1 mmol) for the synthesis of complex **3**. Yield: 73%. Color: Yellow. M.p.: 193 °C. Anal. Calcd for $C_{55}H_{42}As_2O_2N_3RuSCl$: C, 57.65; H, 4.84; N, 6.96; S, 5.31%. Found: C, 57.77; H, 4.94; N, 7.09; S, 5.47%. IR (ATR, cm^{-1}): 3621 (br, ν_{OH}); 1587 + 1478 (m, $\nu_{C=N} + \nu_{C-N}$); 782 (s, ν_{C-S}); 1956 (s, ν_{CO}), ^{1}H NMR (400 MHz, $CDCl_3$, ppm): 10.76 (s, 1H, OH), 9.13 (s, 1H, −CH=N), 7.80 (t, J = 4 Hz, 3H, Ar H), 7.46–7.26 (m, 23H, Ar H), 7.21 (d, J = 4 Hz, 4H, Ar H), 7.03 (d, J = 4 Hz, 2H, Ar H), 6.96 (t, J = 4 Hz, 6H, Ar H), 6.76 (d, J = 8 Hz, 2H, Ar H), ^{13}C NMR (100 MHz, $CDCl_3$, ppm): 205.5 (CO), 166.5 (–HC=N), 157.9 (N=C-N), 148.0 (Ar C), 133.9 (Ar C), 132.8 (Ar C), 130.2 (Ar C), 129.5 (Ar C), 128.2 (Ar C), 127.6 (Ar C), 126.0 (Ar C), 125.8 (Ar C), 125.6 (Ar C), 122.0 (Ar C), 120.2 (Ar C), 118.2 (Ar C), 116.6 (Ar C); 107.3 (Ar C); 142.7–116.6 (Ar C of $AsPh_3$); ESI: *m/z* calcd. for $C_{55}H_{42}As_2O_2N_3RuSCl$, 1095.0; Found, 1096.0 $[M+H]^+$. Single crystals of suitable for X-ray determination were grown by slow evaporation of chloroform-acetonitrile (1:1) solution of complex **3** at room temperature.

2.2.8. X-ray crystallographic study

To collect the data of crystals obtained for complexes **1** and **3**, it should be mounted on glass fiber and then used for further analysis using monochromatic Mo–Kα radiation (λ = 0.71073 Å) in Bruker AXS Kappa APEX II single crystal X-ray diffractometer at 296°(2) K. By using SADABS software, the absorption corrections were done due to Lorentz and polarization effects. To solve the structures of the crystal the least square on F^2 full-matrix was refined by SHELXS-2018 method [30]. The anisotropic property having least squares on F^2 in the weighted full matrix was used to refine the non-hydrogen atoms. The computer programming was already incorporated by the atomic scattering factors.

2.2.9. Common procedure for the α-alkylation of ketone reactions

Ketones (1 mmol), alcohols (1 mmol), catalyst **1** (0.5 mol %), NaOH (5 mol %) and toluene (2 mL) were added into a round bottom flask under air atmosphere. The reaction mixture was stirred with reflux in an oil bath at 105 °C for 8 h. The progress of the reaction was monitored by TLC. After completion of the reaction, the reaction mixture was cooled to room temperature. The catalyst was separated by addition of dichloromethane and petroleum ether solvents mixture (1:1 v/v, 10 mL) followed by filtration through celite. The filtrate was concentrated under reduced pressure and the resulting crude product was purified by column chromatography over silica gel (100–200 mesh) using eluents petroleum ether and ethyl acetate (95:5, v/v) to afford the corresponding ketone. The resulting products were identified by comparison of the ^{1}H & ^{13}C NMR data of previous reports.

3. Results and discussion

3.1. Synthesis of ruthenium(II) complexes

The Schiff base ligands SAL-HBT, VAN-HBT or NAP-HBT were obtained from the reaction of 2-hydrazino benzothiazole with salicylaldehyde, *o*-vanillin or 2-hydroxy-1-naphthaldehyde in ethanol. The Schiff base ligands were reacted with precursor complex [RuHCl(CO)($AsPh_3$)$_3$] in ethanol-chloroform (20 mL, 1:1 v/v) mixture for the synthesis of new complexes (**1–3**) as shown in Scheme 1. In solid state all the complexes are air stable, non-hygroscopic and soluble in common organic solvents such as acetone, benzene, chloroform, dichloromethane, dimethylsulfoxide, dimethyl formamide, ethanol, methanol and insoluble in diethyl ether, hexane and petroleum ether. The formation of the complexes have been confirmed by satisfactory elemental analyses, IR, (^{1}H, ^{13}C) NMR and ESI-mass spectral studies. Moreover, single crystal X- ray analysis was used to confirm the solid-state structure of the complexes (**1** and **3**).

The results of micro analyses (C, H, N and S) of the new complexes (**1–3**) were in fine agreement with the expected structure of the ruthenium hydrazone complexes. The ESI mass spectra of ligands SAL-HBT, VAN-HBT or NAP-HBT and complexes (**1–3**) (Figs. S1-S6 in the supporting information) show the observed molecular ion peaks are in good agreement with their expected molecular masses. Moreover, formation of the intended compounds was strongly supported by the observed fragmentation patterns in their mass spectra.

3.2. IR spectra

The information about the bonding between ligands and the ruthenium metal in the synthesized complexes were predicted using IR spectra. A broad band corresponding to a ν_{OH} vibration that appeared at 3349–3635 cm^{-1} in the spectra ligands was completely disappeared in the spectra of complex **1** and **2**, indicates the involvement of phenolic oxygen in coordination with ruthenium metal. However, in the spectrum of complex **3**, –OH peak was observed at 3621 cm^{-1} reveals the

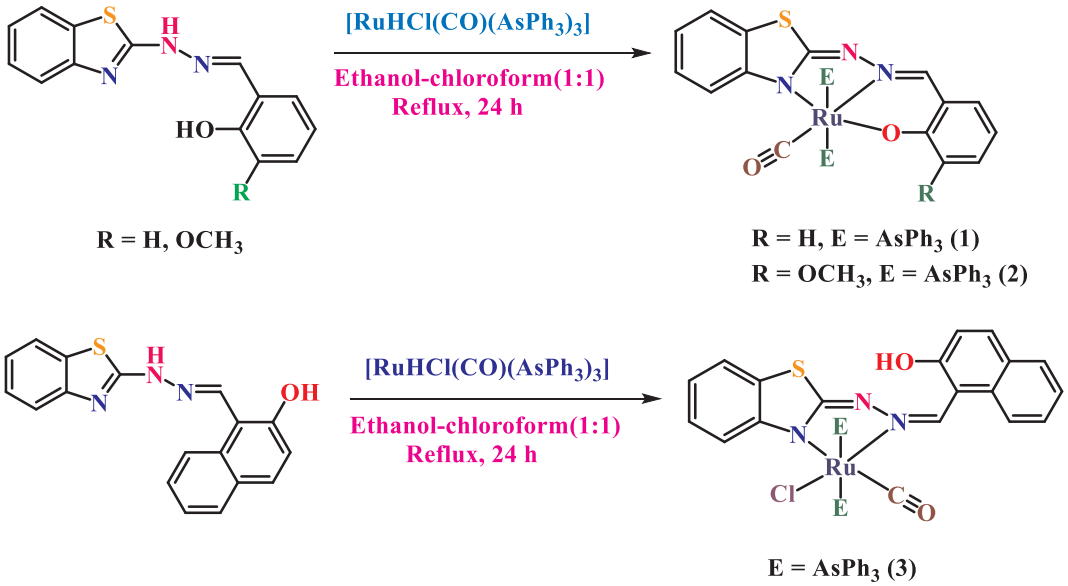

Scheme 1. Synthesis of ruthenium(II) complexes (**1–3**).

non participation of the phenolic oxygen atom in coordination [31]. The spectra of ligands show a peak at 3066–3145 cm^{-1} corresponding to ν_{NH}. On complexation, the ν_{NH} peak disappeared indicate –NH-C=N- ↔ –N=C-NH– tautomerism followed by deprotonation at benzothiazole ring nitrogen and coordination with metal. The presence of strong peak at 1573–1609 cm^{-1} in the spectra of ligands was assigned to imine group. However, in the spectra of complexes, the peak moved to lower frequency and appeared at 1561–1596 cm^{-1} shows the participation of azomethine nitrogen in bonding with metal [32]. Further, all the complexes display a medium to strong band in the region 1948–1956 cm^{-1} corresponding to terminally coordinated carbonyl group which is observed at a slightly higher frequency than in the precursor complexes [33].

3.3. NMR spectra

The formation of compounds as well as the coordination of ligands with the ruthenium metal was established by ^{1}H NMR spectroscopy (Figs. S7-S12 in the supporting information). ^{1}H NMR analyses of all the compounds were done in deuterated solvent at room temperature. The spectra of the free ligands show a singlet at 10.65–11.04 ppm for –OH proton. In the spectra of complexes **1** and **2**, –OH proton peak completely disappeared indicates the involvement of phenolic oxygen in coordination with metal. On the other hand, the –OH peak not disappeared in the spectrum of complex **3**. The complex displays peak in the region 10.76 ppm shows the non coordination of phenolic –OH group with metal in complex **3** [34]. The imine proton of ligands exhibits a singlet at around 8.10–8.39 ppm which is shifted to downfield and appears at 8.16–9.13 ppm in the spectra of all complexes reveals the coordination of imine nitrogen with ruthenium metal. The appearance of peak at 4.25–4.51 ppm in the ligands spectra was assigned to NH proton. The disappearance of NH proton signal in the spectra of complexes (**1–3**) indicates –NH-C=N- ↔ –N=C-NH– tautomerism followed by deprotonation at benzothiazole ring nitrogen during the coordination with metal. The methoxy (OCH_3) protons signal of ligand and complex **2** were observed at 3.93 and 3.86 ppm respectively. Aromatic protons appeared in the region 6.09–7.87 ppm as multiplets in the spectra of complexes and ligands [35].

The ^{13}C NMR spectra of complexes **1–3** further support the formation of proposed complexes and the spectra show the expected signals in the appropriate regions (Figs. S13-S18 in the supporting information). The appearance of peak at 205.2–205.5 ppm reveals the coordinated terminal carbonyl group. The peak for azomethine carbon appears around 164.4–166.5 ppm in the spectra of complexes (**1–3**). The peak due to N=C-N carbon appears at 155.3–165.1 ppm. The methoxy (OCH_3) carbon signal was observed around 56.1 ppm for complex **2**. The aromatic carbons show signals in the region 112.6–148.0 ppm [36].

3.4. Molecular structures of complexes *1* and *3*

Structures of the newly synthesized complexes **1** and **3** have been established by single crystal X-ray diffraction method and the ORTEP drawings are shown in Figs. 1 and 2. The details concerning the data collection and structure refinement of the complexes are summarized in

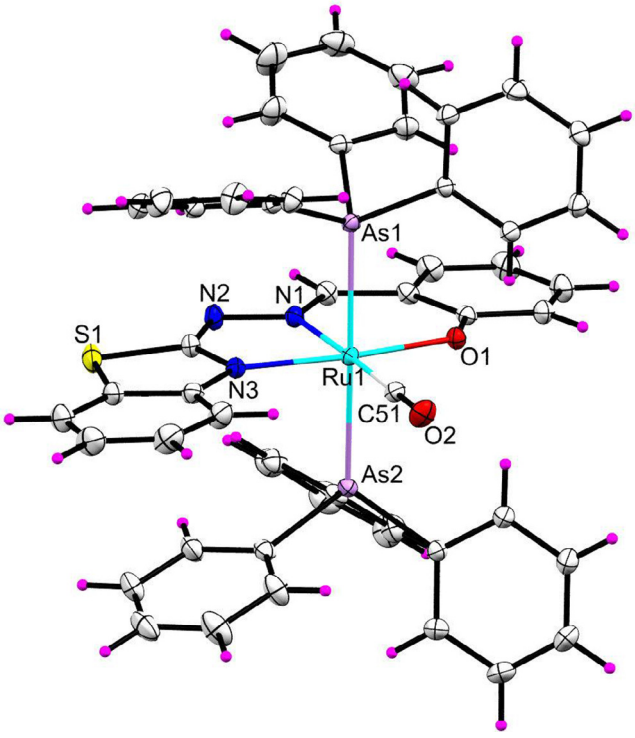

Fig. 1. Perspective view (10% probability ellipsoids) of complex **1**.

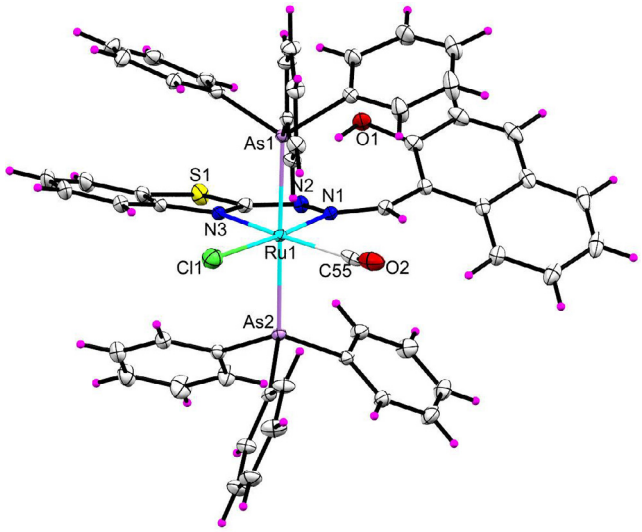

Fig. 2. Perspective view (10% probability ellipsoids) of complex **3**.

Table 1
Crystal data and structural refinement parameters for complexes **1** and **3.**

	1	3
CCDC Number	1999571	1995980
Identification code	shelx	shelx
Empirical formula	$C_{51}H_{39}As_2N_3O_2RuS$	$C_{55}H_{42}As_2ClN_3O_2RuS$
Formula weight	1008.82	1095.34
Temperature (K)	296(2)	296(2)
Wavelength (Å)	0.71073	0.71073
Crystal system	Monoclinic	Monoclinic
Space group	$P2_1/n$	$P2_1/n$
Unit cell dimensions		
a (Å)	11.8308(2)	12.2867(4)
b (Å)	25.8399(5)	20.5946(7)
c (Å)	15.0943(3)	18.8494(6)
α (°)	90	90
β (°)	108.415(10)	91.844(2)
γ (°)	90	90
Volume (Å^3)	4378.14(14)	4767.2(3)
Z	4	4
Density (calculated) Mg/m^3	1.531	1.526
Absorption coefficient (mm^{-1})	1.950	1.852
F(000)	2032	2208
Crystal size (mm^3)	0.22 × 0.20 × 0.18	0.21 × 0.11 × 0.06
Theta range for data collection	2.952 to 28.290°.	1.054 to 29.077°
Index ranges	$-15 \le h \le 15$, $-33 \le k \le 33$, $-18 \le l \le 18$	$-16 \le h \le 16$, $-28 \le k \le 28$, $-25 \le l \le 25$
Reflections collected	24,188	80,783
Independent reflections	10,877 [R(int) = 0.0197]	12,776 [R(int) = 0.0391]
Completeness to theta = 25.242°	98.7%	99.9%
Absorption correction	None	None
Refinement method	Full-matrix least-squares on F^2	Full-matrix least squares on F^2
Data/restraints/parameters	10,747/0/541	12,702/0/586
Goodness-of-fit on F^2	0.846	0.824
Final R indices [I > 2sigma(I)]	R1 = 0.0292, wR2 = 0.0704	R1 = 0.0446, wR2 = 0.1191
R indices (all data)	R1 = 0.0446, wR2 = 0.0865	R1 = 0.0748, wR2 = 0.1615
Largest diff. peak and hole e.Å^{-3}	0.553 and −0.444	1.268 and −1.295

Table 2
Selected bond length and bond angle in complexes **1** and **3.**

1		3	
Inter atomic distance (Å)			
Ru(1)-N(3)	2.0656(17)	Ru(1)-N(1)	2.083(3)
Ru(1)-N(1)	2.0571(18)	Ru(1)-N(3)	2.121(3)
Ru(1)-C(51)	1.863(2)	Ru(1)-C(55)	2.148(11)
Ru(1)-O(1)	2.0705(14)	Ru(1)-Cl(1)	2.4180(19)
Ru(1)-As(1)	2.4633(3)	Ru(1)-As(1)	2.4724(5)
Ru(1)-As(2)	2.4800(3)	Ru(1)-As(2)	2.4849(5)
As(2)-C(39)	1.935(2)	As(2)-C(25)	1.943(4)
As(2)-C(45)	1.948(2)	As(2)-C(31)	1.947(4)
As(2)-C(33)	1.950(2)	As(2)-C(19)	1.951(4)
As(1)-C(15)	1.937(2)	As(1)-C(43)	1.941(4)
As(1)-C(27)	1.942(2)	As(1)-C(49)	1.936(4)
As(1)-C(21)	1.954(2)	As(1)-C(37)	1.950(4)
S(1)-C(14)	1.738(3)	S(1)-C(18)	1.734(6)
S(1)-C(8)	1.759(2)	S(1)-C(12)	1.738(4)
O(2)-C(51)	1.141(3)	C(55)-O(2)	0.577(15)
N(3)-C(9)	1.395(3)	N(1)-C(11)	1.297(5)
N(1)-N(2)	1.401(2)	N(1)-N(2)	1.396(5)
O(1)-C(1)	1.309(3)	O(1)-C(9)	1.339(6)
N(2)-C(8)	1.311(3)	N(2)-C(12)	1.332(6)
N(1)-C(7)	1.287(3)	N(3)-C(12)	1.327(6)
N(3)-C(8)	1.346(3)	N(3)-C(13)	1.397(5)
Bond angles (°)			
C(51)-Ru(1)-N(1)	176.66(8)	C(55)-Ru(1)-N(3)	170.2(3)
C(51)-Ru(1)-N(3)	99.27(9)	C(55)-Ru(1)-N(1)	93.3(3)
N(1)-Ru(1)-N(3)	77.49(7)	N(3)-Ru(1)-N(1)	77.17(13)
C(51)-Ru(1)-O(1)	92.34(8)	C(55)-Ru(1)-Cl(1)	93.0(3)
N(1)-Ru(1)-O(1)	90.92(7)	N(3)-Ru(1)-Cl(1)	96.53(11)
N(3)-Ru(1)-O(1)	168.36(7)	N(1)-Ru(1)-Cl(1)	173.70(10)
C(51)-Ru(1)-As(2)	91.85(7)	C(55)-Ru(1)-As(2)	88.4(3)
N(1)-Ru(1)-As(2)	88.94(5)	N(3)-Ru(1)-As(2)	88.92(10)
N(3)-Ru(1)-As(2)	89.44(5)	N(1)-Ru(1)-As(2)	87.89(10)
O(1)-Ru(1)-As(2)	89.27(4)	Cl(1)-Ru(1)-As(2)	92.03(4)
C(51)-Ru(1)-As(1)	91.41(7)	C(55)-Ru(1)-As(1)	91.9(3)
N(1)-Ru(1)-As(1)	87.85(5)	N(3)-Ru(1)-As(1)	90.44(10)
N(3)-Ru(1)-As(1)	90.98(5)	N(1)-Ru(1)-As(1)	90.07(10)
O(1)-Ru(1)-As(1)	89.64(4)	Cl(1)-Ru(1)-As(1)	89.98(4)
N(2)-N(1)-Ru(1)	116.99(14)	N(2)-N(1)-Ru(1)	115.4(2)
As(1)-Ru(1)-As(2)	176.597(11)	As(2)-Ru(1)-As(1)	177.951(19)

Table 1. Selected bond distances and bond angles with geometrical parameters that are essential for discussion are depicted in Table 2. The single-crystal X-ray studies revealed that complex 1 is crystallized in a monoclinic system with the space group $P2_1/n$ whereas complex 3 crystallized in the monoclinic system belongs to the $P2_1/n$ space group with 4 independent molecules within the unit cell. In complex **1**, the hydrazone ligand coordinated to ruthenium in an ONN fashion by utilizing its phenolic oxygen, benzothiazole ring nitrogen and imine nitrogen with the formation of one six-membered ring and another five membered ring with a N(1)-Ru(1)-N(3) bite angle of 77.49(7)° (Fig. 1). However, in comparison with complex **3**, the angular distortion observed in **1** is significantly less, which may be due to the strong ONN chelation of the ligand. The Ru(1)-N(1) and Ru(1)-N(3) bond distances were found to be 2.0571(18) Å and 2.0656(17) Å, respectively. The other three sites are occupied by triphenylarsine with Ru(1)-As(1) and Ru(1)-As(2) distances of 2.4633(3) and 2.4800(3) Å, respectively, and one carbonyl group with a Ru(1)-C(51) distance of 1.863(2) Å. These values are comparable with those found for complexes reported previously [37]. N(1)-Ru(1)-As(2) 88.94(5)°, N(3)-Ru(1)-As(2) 89.44(5)°, O(1)-Ru(1)-As(2) 89.27(4)°, N(1)-Ru(1)-As(1) 87.85(5)°, O(1)-Ru(1)-As(1) 89.64(4)° cis angles are more acute than 90°, whereas the other cis angles, C(51)-Ru(1)-N(3) 99.27(9)°, C(51)-Ru(1)-O(1) 92.34(8)°, N(1)-Ru(1)-O(1) 90.92(7)°, C(51)-Ru(1)-As(2) 91.85(7)°, C(51)-Ru(1)-As(1) 91.41(7)°, N(3)-Ru(1)-As(1) 90.98(5)° are more obtuse than 90°. The trans angles O(1)-Ru(1)- N(3) 168.36(7)°, C(51)-Ru(1)-N(1) 176.66(8)° and As(1)-Ru-As(2) 176.597(11)° show some degree of deviation from the ideal geometry. The deviation in bond angles and the variations in

bond lengths indicate distortion in the octahedral symmetry of the complexes.

In complex **3**, the ruthenium(II) ion exhibits a hexa coordination with an distorted octahedral geometry where equatorial coordination comes from benzothiazole ring nitrogen and imine nitrogen of bidentate chelating ligand, a chloride and a carbonyl carbon. A pair of triphenylarsines completes the axial coordination (Fig. 2). The hydrazone ligand coordinated to ruthenium and form a five membered ring with a N(1)–Ru(1)–N(3) bite angle of 77.17(13)°. The Ru(1)–N(1) and Ru(1)–N(3) bond distances are 2.083(3) Å and 2.121(3) Å respectively. The other four sites are occupied by two triphenylarsine ligands, which are mutually trans to each other with Ru(1)–As(1) and Ru(1)–As(2) distances of 2.4724(5) and 2.4849(5) Å, and one chloride and a carbonyl group with Ru(1)–Cl(1) and Ru(1)–C(55) distances of 2.4180(19) and 2.148(11) Å, respectively. The N(1)–Ru(1)–As(2) 87.89(10)°, N(3)-Ru(1)-As(2) 88.92(10)°, C(55)-Ru(1)-As(2) 88.4(3)°, Cl(1)-Ru(1)-As(1) 89.98(4)° cis angles are more acute than 90°, whereas the other cis angles, C(55)-Ru(1)-N(1) 93.3(3)°, C(55)-Ru(1)-Cl(1) 93.0(3)°, N(3)-Ru(1)-Cl(1) 96.53(11)°, Cl(1)-Ru(1)-As(2) 92.03(4)°, C(55)-Ru(1)-As(1) 91.9(3)°, N(3)-Ru(1)-As(1) 90.44(10)°, N(1)-Ru(1)-As(1) 90.07(10)°, N(2)-N(1)-Ru(1) 115.4(2)° are more obtuse than 90°. The C(55)-Ru(1)-N(3) 170.2(3)°, N(1)-Ru(1)-Cl(1) 173.70(10)°, As(2)-Ru(1)-As(1) 177.951(19)° trans angles significantly deviate from the linearity [38–40]. Generally the $AsPh_3$ ligands usually prefer to occupy mutually cis position for better π-interaction, but in the reported complexes the presence of CO, a stronger π -acidic ligand, might have forced the bulky $AsPh_3$ ligands to take trans position for steric reasons [41,42].

3.5. Catalytic studies

3.5.1. Optimization of reaction conditions

Recently, the core moiety of the pharmaceutically active intermediate was successively synthesized through hydrogen auto-transfer process via alkylation using homogeneous catalysts [24,43]. Hence, we are interested to assess the catalytic efficiency of Ru(II) hydrazone complexes in the synthesis of pharmaceutical compounds with C–C bond by cross coupling of ketones and alcohols known as α-alkylation reactions. To optimize the best catalytic reaction conditions, we consider the formation of benzylated acetophenone as a benchmark substrate from the reaction of acetophenone with benzyl alcohol in the presence of Ru(II) hydrazone catalyst **1** (0.5 mol%). The effects of the base, temperature, solvent and time were investigated. The results of the preliminary reactions were shown in Table 3. The base plays a key role in this reaction. To determine the role of base, the alkylation reaction was carried out with different bases like $NaHCO_3$, Na_2CO_3, K_2CO_3, KO^{t}Bu, Cs_2CO_3, KOH and NaOH. The results reveal weak bases such as $NaHCO_3$, K_2CO_3, Na_2CO_3, were not effective to accelerate the reaction (Table 3, entries 1, 2 and 3). The bases KO^{t}Bu and Cs_2CO_3 led to moderate yields (Table 3, entries 4 and 5). Especially, strong base like KOH and NaOH have shown good to excellent yields (Table 3, entries 6 and 7). Among the bases enlisted, NaOH (5 mol %) was discovered to be the best base and led to excellent yield in shorter reaction time for this reaction. (Table 3, entry 7, yield 95%).

It was well known that the solvent can have authentic effect on α-alkylation reaction. Accordingly, the solvent-dependent differences in activity of catalyst **1** were studied on the model reaction with frequently used solvents such as toluene, benzene, acetonitrile, 1,4 dioxane, tetrahydrofuran, DMF and DMSO (Table 3, entries 1–18). Among them, polar aprotic solvents like DMSO and DMF invariably give poor yields (Table 3, entries 14 and 15). Ether like solvents such as dioxane, THF afford better yield than polar aprotic solvents (Table 3, entries 12 and 13). Acetonitrile and benzene have shown moderate yields of 80 and 85% respectively in the alkylation reaction (Table 3, Entries 10 and 11). However, toluene was found to be the solvent of choice, bestow excellent yield of 93% in 8 h (Table 3, Entry 8). In addition, when the reactions were conducted in the absence of base, no product was formed (Table 3, entry 17). As expected, no considerable conversion was observed without catalyst under similar reaction conditions after a prolonged reaction time up to 24 h (Table 3, entry 18). Also, decreasing the reaction temperature from 105 to 90 °C led to decrease in yield from 93 to 68% (Table 3, entries 8 and 9). Therefore, 105 °C was considered to be suitable temperature which proved that our catalytic system could achieve the reaction well relatively lower temperature compared to reported work (140 °C) [44]. When the reaction was monitored in shorter time, there is no significant change in yield of the product was observed (Table 3, entry 8). Therefore, the reaction time of 8 h was considered as optimal reaction time to

Table 3
Optimization of catalytic conditions for the α-alkylation of acetophenone using benzyl alcohol.[a]

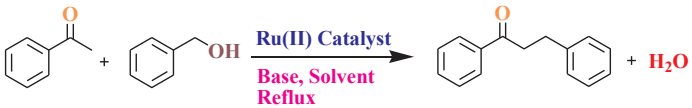

Entry	Base	Solvent	T (°C)	Time (h)	Yield[b] (%)
1	$NaHCO_3$	Toluene	105	24	37
2	K_2CO_3	Toluene	105	24	42
3	Na_2CO_3	Toluene	105	24	50
4	Cs_2CO_3	Toluene	105	24	74
5	KO^{t}Bu	Toluene	105	24	65
6	KOH	Toluene	105	24	78
7	NaOH	Toluene	105	24	95
8	NaOH	Toluene	105	8	93
9	NaOH	Toluene	90	8	68
10	NaOH	Benzene	100	8	85
11	NaOH	CH_3CN	85	8	80
12	NaOH	Dioxane	80	8	72
13	NaOH	THF	70	8	65
14	NaOH	DMSO	130	8	19
15	NaOH	DMF	120	8	25
16	NaOH	Toluene	RT	24	NR
17[c]	_	Toluene	105	24	NR
18[d]	NaOH	Toluene	105	24	NR

[a] Acetophenone (1 mmol), benzyl alcohol (1 mmol), base (5 mol %), catalyst **1** (0.5 mol%), refluxed in solvent (2 mL).
[b] Isolated yield after column chromatography.
[c] The reaction was carried out without base. No reaction.
[d] The reaction was carried out without catalyst. No reaction.

Table 4
Selection of catalyst and influence of catalyst loading on α-alkylation of acetophenone with benzyl alcohol.[a]

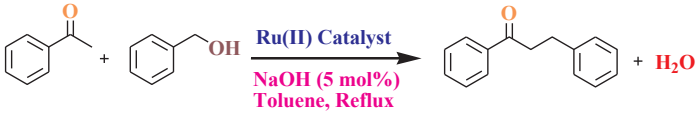

Entry	Catalyst	Amount of catalyst (Mol %)	Yield[b] (%)
1	**1**	**0.5**	**93**
2	2	0.5	82
3	3	0.5	88
4	1	0.1	47
5	1	0.2	65
6	1	0.3	74
7	1	1	95

[a] Acetophenone (1 mmol), benzyl alcohol (1 mmol), catalyst, NaOH (5 mol %) in toluene (2 mL) refluxed at 105 °C for 8 h.
[b] Isolated yield after column chromatography.

Table 5
Scope of the reaction in α-alkylation of ketones.[a]

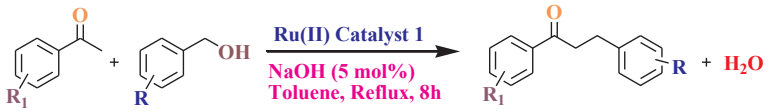

Entry	Ketone	Alcohol	Product	Yield[b]
1	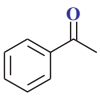	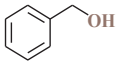	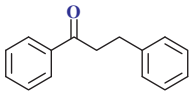 1a	93
2	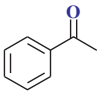	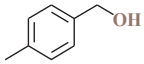	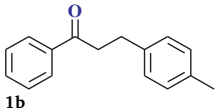 1b	90
3	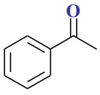	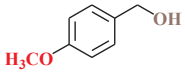	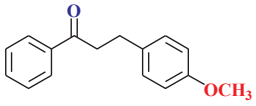 1c	91
4	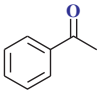	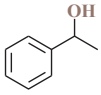	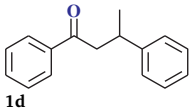 1d	87
5	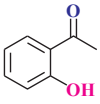	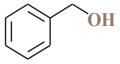	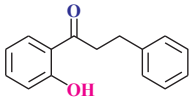 1e	79
6	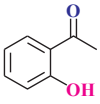	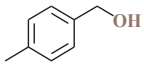	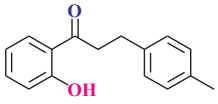 1f	74
7	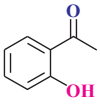	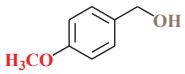	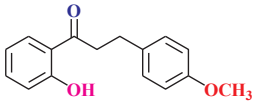 1g	76
8	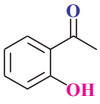	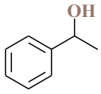	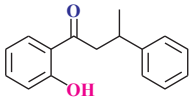 1h	70
9		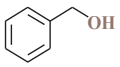	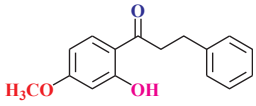 1i	92
10	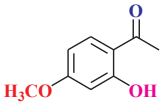	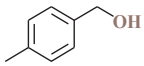	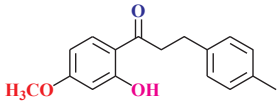 1j	91
11		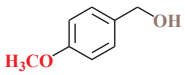	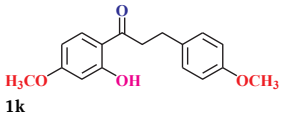 1k	94
12		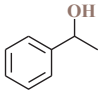	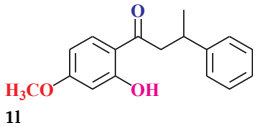 1l	88

(continued on next page)

Table 5 (*continued*)

Entry	Ketone	Alcohol	Product	Yield[b]
13	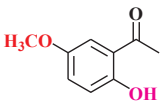	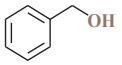	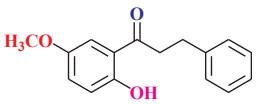 **1m**	86
14	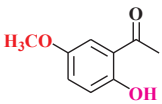	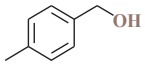	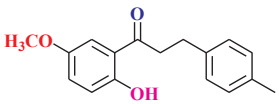 **1n**	82
15	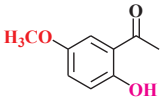	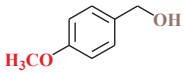	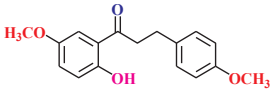 **1o**	84
16	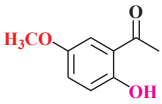	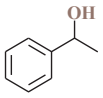	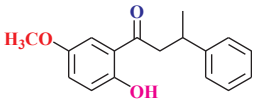 **1p**	80
17		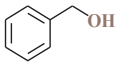	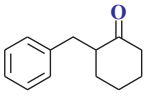 **1q**	81
18		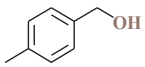	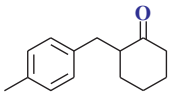 **1r**	87
19		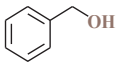	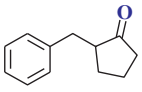 **1s**	83
20		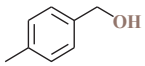	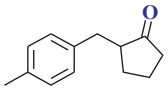 **1t**	80

[a] Ketone (1 mmol), alcohol (1 mmol), catalyst **1** (0.5 mol %) and NaOH (5 mol %) in toluene (2 mL) refluxed at 105 °C for 8 h.
[b] Isolated yield after column chromatography.

complete the alkylation reaction.

The screening reaction was then extended to selection of catalyst and catalytic loading in the alkylation reaction and the results were collated in Table 4. To study the effect of amount of the catalyst, the reactions were carried out at different amount of catalyst ranging from 0.1 to 1.0 mol %. The catalyst loading increased from 0.1 to 0.5 mol% of catalyst **1**, the product yield also increased and reaches 93% in 8 h. Doubling the loading of catalyst **1** (1 mol%) led to little difference in yield (Table 4, entry 6). Hence, the optimum catalyst loading was fixed to be 0.5 mol % (Table 4, entry 1). Additionally, catalyst **1** was found to be the best catalyst for α-alkylation reaction to obtain excellent yield (Table 4, entry 1). Other catalysts such as **2** and **3** show lower activity than the catalyst **1** (Table 4, entry 1 and 2). From the optimization results, it is concluded that 0.5 mol % of catalyst **1** in toluene was sufficient to push this reaction at 105^{0}C in presence of NaOH.

3.5.2. Substrate scope

With the optimized reaction conditions in hand, various primary alcohols were reacted with different types of ketones to examine the scope of the reaction. All reactions resulted in complete conversion of starting materials to afford selective formation of the corresponding ketone (Table 5). Initially, investigation was focused on the α-alkylation of aromatic acetophenone with alcohols like benzyl alcohol, 4-methyl benzyl alcohol, 4-methoxy benzyl alcohol and the reactions give the α-alkylated products in higher yields (Table 5, entries 1–3). However, marginal decrease in yield was observed for the reaction of aromatic acetophenone with electron-rich 1-phenylethanol (Table 5, entry 4). The steric effect due to the presence of hydroxy group in the ortho position of acetophenone affects the product yield and hence the yields are moderate (Table 5, entries 5–8; Yield 70–79%). The reactions of 4-methoxy-2-hydroxy acetophenone with alcohols such as benzyl alcohol, 4-methyl benzyl alcohol, 4- methoxy benzyl alcohol and 1 phenyl ethanol offer corresponding pharmaceutically important C–C coupling products in good to excellent yields (Table 5, entries 9–12; Yield 88–94%). Encouraged by the result, coupling of 5-methoxy-2-hydroxy acetophenone with various alcohols containing electron donating groups were done. The reactions offer the desired products in good yields, however, the yield are lesser than the 4-methoxy-2-hydroxy acetophenone coupling products (Table 5, entries 13–16). The aliphatic cyclic ketones, such as cyclohexanone and cyclopentanone were successfully transformed into the corresponding α-alkylated ketones in good yields (Table 5, entries 17–20). The results show that catalyst **1** was effective in the alkylation of not only aromatic but also aliphatic ketones (Table 5, entries 1–20).

On the basis of the above experimental observations, the complex **1** was proved as effective catalyst for α-alkylation of variety of ketones with primary alcohols under air via environmentally friendly borrowing hydrogen pathway. A plausible mechanism for α-alkylation of ketones

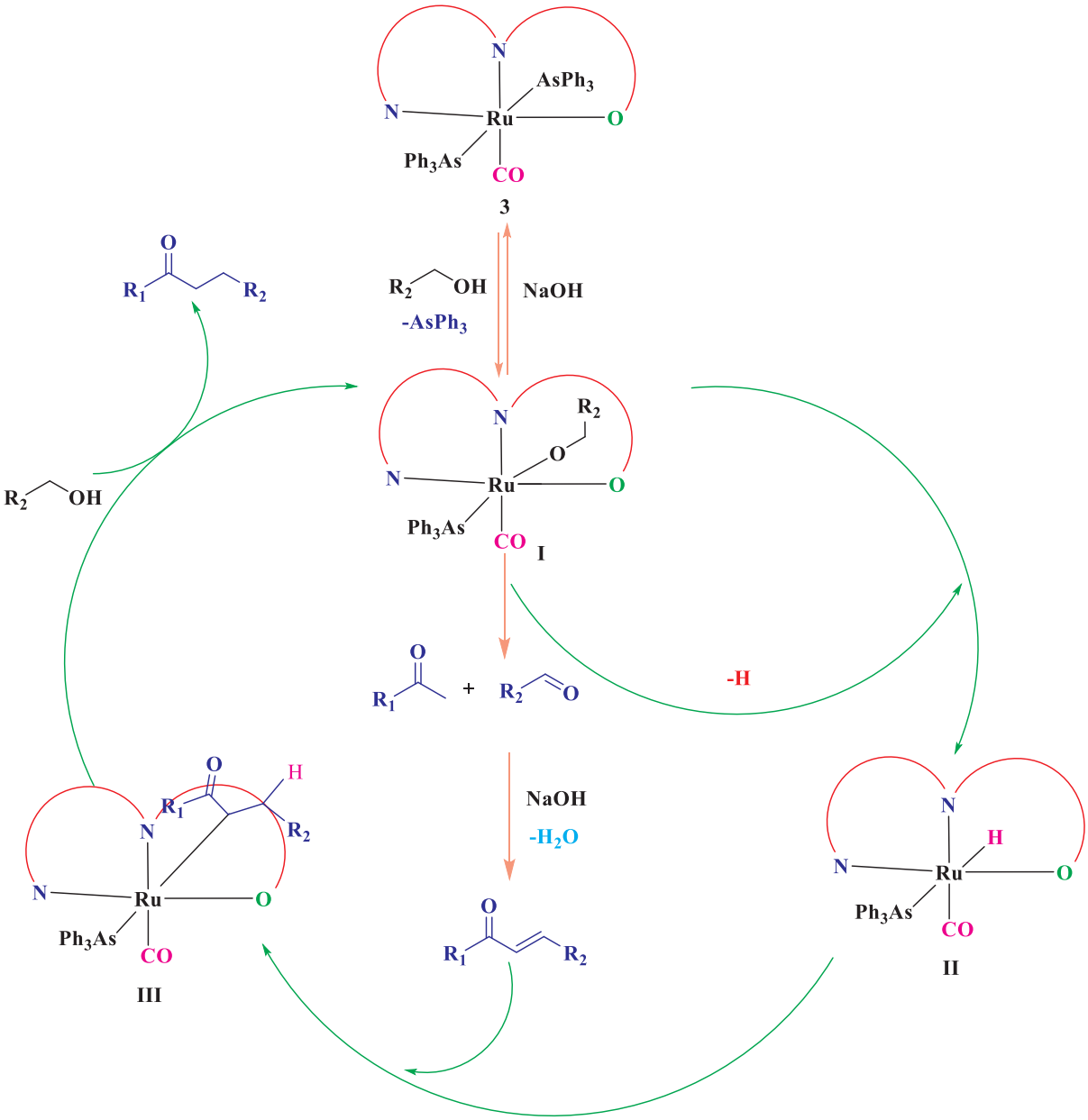

Scheme 2. Proposed plausible mechanism for α-alkylation of ketones with alcohols.

with alcohols catalyzed by complex **1** is shown in Scheme 2. Initially, the reaction between Ru catalyst and alcohol in the presence of base generates Ru-alkoxide species I. Subsequently, β-hydrogen elimination of alkoxo ruthenium species I gives rise to Ru-H species II and the aldehyde intermediate. Although we were unable to isolate R-H species II, the generation of R-H complexes was well documented [45,46] and has been verified by the Yu group [47] as the active catalyst for transfer hydrogenation. Next, the condensation reaction between intermediate aldehyde and ketone in the presence of NaOH results in α,β-unsaturated ketone. Finally, the coordination and addition of Ru-H species II into the double bond of α,β-unsaturated ketone affords Ru species III, which combines with the alcohol to release the ketone product and regenerate Ru-alkoxide species I.

The results of present catalyst were compared with the recent catalysts explored for α-alkylation to reveal the better performance. The previously reported Mn catalyzed [48,49] α-alkylation reactions required high catalyst loading (1–2 mol %), high temperature (125-140 °C) and longer time (18–24 h) for completion of reactions. For effective formation of products, Ru NHC catalyst necessitates [25] 2 mol % catalyst loading and 24 h reaction time at 100 °C. Similarly $[RuCl_2(\eta^6\text{-}p\text{-cymene})]_2$ and P,N ligand catalyst [50] was shown efficient catalytic activity at 120 °C in 18 h. Moreover, NNN pincer Ru(II) complexes and ruthenium pyridonate complexes [26,51] were effective only under inert atmosphere. However, using the present catalyst, the α-alkylation reactions were carried out at relatively low temperature (105 °C) in shorter time (8 h) using minimal catalyst load (0.5 mol %) under air. The results offer new possibilities for developing versatile catalysts for α-alkylation of ketones.

4. Conclusions

A new series of facile Ru(II) complexes (**1–3**) were synthesized by the reaction of $[RuHCl(CO)(AsPh_3)_3]$ with hydrazone ligands (SAL-HBT, VAN-HBT or NAP-HBT). The formation of the complexes was established by analytical and spectral (IR, NMR, and ESI-MS) methods. The solid-state structures reveal the ruthenium(II) ion exhibits a hexa

coordination with distorted octahedral geometry. In complex **1** and **2**, the hydrazone ligand coordinated to ruthenium in a dianionic tridentate ONN fashion by utilizing its phenolic oxygen, benzothiazole ring nitrogen and imine nitrogen with the formation of one six-membered ring and another five membered ring. However, in complex **3**, the ligand coordinated in a monoanionic bidentate NN fashion by forming a five-membered ring. The catalytic effectiveness of the titled complexes was well explored for α-alkylation of a wide range of ketones with primary alcohols via hydrogen borrowing technique with excellent yields. Catalytic reactions were carried out at relatively low temperature in short time with minimal catalyst load (0.5 mol %) under air atmosphere. The results offer new possibilities for developing versatile catalysts for α-alkylation reaction of ketones using alcohols.

CRediT authorship contribution statement

Subbarayan Vijayapritha: Conceptualization, Investigation, Writing - original draft. **Kaliyappan Murugan:** Visualization. **Periasamy Viswanathamurthi:** Methodology, Validation, Supervision, Project administration. **Paranthaman Vijayan:** Software, Visualization, Resources. **Chinnasamy Kalaiarasi:** Software, Visualization.

Declaration of Competing Interest

The authors declare that they have no known competing financial interests or personal relationships that could have appeared to influence the work reported in this paper.

Acknowledgements

We thank SAIF, Punjab University, Chandigarh, Department of Chemistry, Gandhigram Rural Institiue, Gandhigram (spectral studies) and CIMF, Periyar University, Salem (single crystal X-Ray) for their help in characterization studies.

Appendix A. Supplementary data

CCDC 1999571 and 1995980 contain the supplementary crystallographic data for complexes **1** and **3**. This data can be obtained free of charge via http://www.ccdc.cam.ac.uk/conts/retrieving.html, or from the Cambridge Crystallographic Data Centre, 12 Union Road, Cambridge CB2 1EZ, UK; fax: (+44) 1223-336-033; or email: deposit@ccdc.cam.ac.uk. Supplementary data to this article can be found online at https://doi.org/10.1016/j.ica.2020.119887.

References

[1] (a) P.K. Suganthy, R.N. Prabhu, V.S. Sreedevi, Tetrahedron Lett. 54 (2013) 5695;
(b) P.R. Verma, S. Mandal, P. Gupta, B. Mukhopadhyay, Tetrahedron Lett. 54 (2013) 4914;
(c) S. Datta, D.K. Seth, S. Gangopadhyay, P. Karmakar, S. Bhattacharya, Inorg. Chim. Acta 392 (2012) 118;
(d) P. Paul, S. Datta, S. Halder, R. Acharyya, F. Basuli, R.J. Butcher, S.M. Peng, G.H. Lee, A. Castineiras, M.G.B. Drew, S. Bhattacharya, J. Mol. Catal. A: Chem. 344 (2011) 62.
[2] G. Xie, P. Chellan, J. Mao, K. Chibale, G.S. Smith, Adv. Synth. Catal. 352 (2010) 1641.
[3] (a) J. Dutta, S. Bhattacharya, RSC Adv. 3 (2013) 10707;
(b) J. Dutta, S. Datta, D. Kumar Seth, S. Bhattacharya, RSC Adv. 2 (2012) 1175;
(c) P. Pelagatti, A. Venturini, A. Leporati, M. Carcelli, M. Costa, A. Bacchi, G. Pelizzi, C. Pelizzi, J. Chem. Soc. Dalton Trans. 13 (1998) 2715.
[4] U. Abram, K. Ortner, R. Gust, K. Sommer, J. Chem. Soc. Dalton Trans. 5 (2000) 735.
[5] G. Argay, A. Kalman, L. Parkanyi, V.M. Leovac, I.D. Brceski, P.N. Radivojsa, J. Coord. Chem. 51 (2000) 9.
[6] A. Castineiras, R. Pedrido, Dalton Trans. 41 (2012) 1363.
[7] (a) T.S. Lobana, R. Sharma, G. Bawa, S. Khanna, Coord. Chem. Rev. 253 (2009) 977;
(b) T.S. Lobana, G. Bawa, A. Castineiras, R.J. Butcher, M. Zeller, Organometallics 27 (2008) 175;
(c) T.S. Lobana, G. Bawa, R.J. Butcher, Inorg. Chem. 47 (2008) 1488;
(d) R. Archaryya, F. Basuli, S.M. Peng, G.H. Lee, L.R. Falvello, S. Bhattacharya, Inorg. Chem. 45 (2006) 1252;
(e) I. Pal, F. Basuli, T.C.W. Mak, S. Bhattacharya, Angew. Chem. Int. Ed. 113 (2001) 3007;
(f) J.S. Casas, M.S.G. Tasende, J. Sordo, Coord. Chem. Rev. 209 (2000) 197;
(g) S. Padhi, G.B. Kauffman, Coord. Chem. Rev. 63 (1985) 127;
(h) M.J.M. Campbell, Coord. Chem. Rev. 15 (1975) 297.
[8] (a) S. Dharani, G. Kalaiarasi, D. Sindhuja, V.M. Lynch, R. Shankar, R. Karvembu, R. Prabhakaran, Inorg. Chem. 58 (2019) 8045;
(b) A. Najafian, T.R. Cundari, Inorg. Chem. 58 (2019) 12254;
(c) S. Shaw, J.D. White, Chem. Rev. 119 (2019) 9381;
(d) G. Occhipinti, V.R. Jensen, H. Bjorsvik, J. Org. Chem. 72 (2007) 3561;
(e) A. Martinez, C. Hemmert, C. Loup, G. Barré, B. Meunier, J. Org. Chem. 71 (2006) 1449.
[9] (a) D. Palanimuthu, S.V. Shinde, K. Somasundaran, A.G. Samuelson, J. Med. Chem. 56 (2013) 722;
(b) J.L. Hickey, P.S. Donnelly, Coord. Chem. Rev. 256 (2012) 2367;
(c) P.V. Bernhardt, P.C. Sharpe, M. Islam, D.B. Lovejoy, D.S. Kalinowski, D.R. Richardson, J. Med. Chem. 52 (2009) 407;
(d) A.G. Quiroga, C.N. Ranninger, Coord. Chem. Rev. 248 (2004) 119.
[10] L. Dkhar, W. Kaminsky, K. Mohan Poluri, M.R. Kollipara, J. Organomet. Chem. 891 (2019) 54.
[11] T.S. Lobana, G. Bawa, R.J. Butcher, B.J. Liaw, C.W. Liu, Polyhedron 25 (2006) 2897.
[12] (a) S.A. Lawerencem, Amine: Synthesis Properties and Applications, Cambridge University, Cambridge, 2004;
(b) K.P.C. Vollhardt, N.E. Schore, Organic Chemistry: Structure and function, 5th edn, W. H. Freeman, New York, 2007;
(c) A.R. Katritzky, C.W. Rees, Comprehensive Heterocyclic. Chemistry II, (Ed.), Elsevier, Oxford, 1996.
(d) J. Leonard, A. Blacker, S.P. Marsden, M.F. Jones, K.R. Mulholl, R. Newton, Org. Process Res. Dev. 19 (2015) 1400
[13] (a) G. Casiraghi, L. Battistini, C. Curti, G. Rassu, F. Zanardi, Chem. Rev. 111 (2011) 3076;
(b) C. Palomo, M. Oiarbide, J.M. Garcia, Chem. Soc. Rev. 33 (2004) 65;
(c) P. Arya, H. Qin, Tetrahedron 56 (2000) 917.
[14] (a) J. Mlynarski, B. Gut, Chem. Soc. Rev. 41 (2012) 587;
(b) P.H.Y. Cheong, C.Y. Legault, J.M. Um, N. Celebi-Olcum, K.N. Houk, Chem. Rev. 111 (2011) 5042.
[15] Y. Obora, ACS Catal. 4 (2014) 3972.
[16] (a) S. Thiyagarajan, C. Gunanathan, ACS Catal. 7 (2017) 5483;
(b) A. Corma, J. Navas, M.J. Sabater, Chem. Rev. 11 (2018) 1410;
(c) Y. Liu, A. Afanasenko, S. Elangovan, Z. Sun, K. Barta, ACS Sustainable Chem. Eng. 7 (2019) 11267;
(d) T. Irrgang, R. Kempe, Chem. Rev. 119 (2019) 2524.
[17] J.F. Jenck, F. Agterberg, M.J. Droescher, Green Chem. 6 (2004) 544–556.
[18] A.K. Bains, A. Kundu, S. Yadav, D. Adhikari, ACS Catal. 9 (2019) 9051.
[19] R. Grigg, T.R.B. Mitchell, S. Sutthivaiyakit, N. Tongpenyai, Tetrahedron Lett. 22 (1981) 4107.
[20] (a) C.S. Cho, B.T. Kim, T.-J. Kim, S.C. Shim, J. Org. Chem. 66 (2001) 9020;
(b) C.S. Cho, B.T. Kim, T.-J. Kim, S.C. Shim, Tetrahedron Lett. 43 (2002) 7987;
(c) R. Martinez, D.J. Ramon, M. Yus, Tetrahedron 62 (2006) 8988;
(d) T. Kuwahara, T. Fukuyama, I. Ryu, Org. Lett. 14 (2012) 4703;
(e) R. Martinez, G.J. Brand, D.J. Ramon, M. Yus, Tetrahedron Lett. 46 (2005) 3683;
(f) F. Alonso, F. Foubelo, J.C. Gonzalez-Gomez, R. Martinez, D.J. Ramon, P. Riente, M. Yus, Mol. Diversity 14 (2010) 411;
(g) K. Taguchi, H. Nakagawa, T. Hirabayshi, S. Sakaguchi, Y. Ishii, J. Am. Chem. Soc. 126 (2004) 72;
(h) G. Onodera, Y. Nishibayashi, S. Uemura, Angew. Chem. Int. Ed. 45 (2006) 3819;
(i) M. Rueping, V.B. Phapale, Green Chem. 14 (2012) 55;
(j) S. Bhat, V. Scridharan, Chem. Commun. 48 (2012) 4701;
(k) R. Kawahara, K.-I. Fujita, R. Yamaguchi, J. Am. Chem. Soc. 132 (2010) 15108;
(l) H. Aramoto, Y. Obora, Y. Ishii, J. Org. Chem. 74 (2009) 628;
(m) C.S. Cho, J. Mol. Catal. A 240 (2005) 55.
[21] (a) K. Motokura, D. Nishimura, K. Mori, T. Mizugaki, K. Ebitani, K. Kaneda, J. Am. Chem. Soc. 126 (2004) 5662;
(b) K. Motokura, N. Fujita, K. Mori, T. Mizugaki, K. Ebitani, K. Jitsukawa, K. Kaneda, Chem. - Eur. J. 12 (2006) 8228.
[22] H.W. Cheung, J. Li, W. Zheng, Z. Zhou, Y.H. Chiu, Z. Lin, C.P. Lau, Dalton Trans. (2010) 265.
[23] F.X. Yan, M. Zhang, X. Wang, F. Xie, M. Chen, H. Jiang, Tetrahedron 70 (2014) 1193.
[24] X. Cao, X. Wan, F. Yang, K. Li, X. Hao, T. Shao, X. Zhu, M. Song, J. Org. Chem. 83 (2018) 3657.
[25] C. Schlepphorst, B. Maji, F. Glorius, ACS Catal. 6 (2016) 4184.
[26] C. Zhang, J. Zhao, B. Hu, J. Shi, D. Chen, Organometallics 38 (2019) 654.
[27] (a) R. Ramachandran, G. Prakash, S. Selvamurugan, P. Viswanathamurthi, J.G. Malecki, V. Ramkumar, Dalton Trans. 43 (2014) 7889;
(b) R. Ramachandran, P. Viswanathamurthi, Spectrochim. Acta Part A 103 (2014) 53;
(c) G. Prakash, R. Ramachandran, M. Nirmala, P. Viswanathamurthi, W. Linert, Monatsh. Chem. 145 (2014) 1903;
(d) G. Prakash, P. Viswanathamurthi, Spectrochim. Acta Part A 129 (2014) 352.
[28] L. Dkhar, W. Kaminsky, K.M. Poluri, M.R. Kollipara, J. Orgmet. Chem. 891 (2019) 54.

[29] A. Sanchez-Delgado, W.Y. Lee, S.R. Choi, Y. Cho, M.J. Jun, Trans. Met. Chem. 16 (1991) 241.
[30] G.M. Sheldrick, Acta. Crystallogr. Sect. A 64 (2008) 112.
[31] R. Prabhakaran, P. Kalaivani, R. Jayakumar, M. Zeller, A.D. Hunter, S.V. Renukadevi, E. Ramachandran, K. Natarajan, Metallomics 3 (2011) 42.
[32] A. Castineiras, R. Pedrido, Inorg. Chem. 48 (2009) 4847.
[33] P. Kalaivani, R. Prabhakaran, E. Vaishnavi, B.T. Rueffer, H. Lang, P. Poornima, R. Renganathan, V. Vijaya Padma, K. Natarajan, Inorg. Chem. Front. 1 (2014) 311.
[34] P. Kalaivani, R. Prabhakaran, F. Dallemer, E. Vaishnavi, P. Poornima, V. Vijaya Padma, R. Renganathan, K. Natarajan, J. Organomet. Chem. 762 (2014) 67.
[35] S. Selvamurugan, R. Ramachandran, G. Prakash, M. Nirmala, P. Viswanathamurthi, S. Fujiwara, A. Endo, Inorg. Chim. Acta 454 (2017) 46.
[36] R. Ramachandran, G. Prakash, M. Nirmala, P. Viswanathamurthi, J.G. Malecki, W. Linert, A. Gusev, RSC Adv. 5 (2015) 11405.
[37] P. Kalaivani, R. Prabhakaran, P. Poornima, F. Dallemer, K. Vijayalakshmi, V. Vijaya Padma, K. Natarajan, Organometallics 31 (2012) 8323.
[38] P. Vijayan, P. Viswanathamurthi, V. Silambarasan, D. Velmurugan, K. Velmurugan, R. Nandhakumar, R.J. Butcher, T. Silambarasan, R. Dhandapani, J. Organomet. Chem. 768 (2014) 163.
[39] R. Prabhakaran, P. Kalaivani, R. Huang, M. Sieger, W. Kaim, P. Viswanathamurthi, F. Dallemer, K. Natarajan, Inorg. Chim. Acta 376 (2011) 317.
[40] P. Vijayan, P. Viswanathamurthi, P. Sugumar, M.N. Ponnuswamy, M.D. Balakumaran, P.T. Kalaichelvan, K. Velmurugan, R. Nandhakumar, R.J. Butcher, Inorg. Chem. Front. 2 (2015) 620.
[41] J.G. Malecki, A. Maron, M. Serda, J. Polanski, Polyhedron 56 (2013) 44.
[42] P. Kalaivani, R. Prabhakaran, P. Poornima, R. Huang, V. Hornebecq, F. Dallemer, V. Vijaya Padma, K. Natarajan, RSC Adv. 3 (2013) 20363.
[43] G. Balamurugan, S. Balaji, R. Ramesh, N.S.P. Bhuvanesh, Appl. Organometal. Chem. (2018) e4696.
[44] T. Kuwahara, T. Fukuyama, I. Ryu, Org. Lett. 14 (2012) 4703.
[45] (a) T. Li, R. Churlaud, A.J. Lough, K. Abdur-Rashid, R.H. Morris, Organometallics 23 (2004) 6239;
(b) F. Zeng, Z. Yu, Organometallics 27 (2008) 2898.
[46] X. Wan, Z. Liu, W. Liu, X. Cao, X. Zhus, X. Zhao, B. Song, X. Hao, G. Liu, Tetrahedron 75 (2019) 2697.
[47] W. Du, P. Wu, Q. Wang, Z. Yu, Organometallics 32 (2013) 3083.
[48] S.S. Gawali, B.K. Pandia, S. Pal, C. Gunanathan, ACS Omega 4 (2019) 10741.
[49] S. Chakraborty, P. Daw, Y.B. David, D. Milstein, ACS Catal. 8 (2018) 10300.
[50] S. Liu, L. Xu, C. Liu, Z. Ren, D.J. Young, J. Lang, Tetrahedron 73 (2017) 2374.
[51] Z. Zhu, Y. Li, Y. Wang, Z. Lan, X. Zhu, X. Hao, M. Song, Organometallics 38 (2019) 2156.